International Journal of Technology

http://ijtech.eng.ui.ac.id

Research Article

Facile Synthesis and Characterization of Magnetite Mesoporous Silica Nanoparticles from Local Iron Sand

Mita Kurniasari [1], Himawan Tri Bayu Murti Petrus [1,2], Siti Nurul Aisyiyah Jenie [3], Yuni Kusumastuti [1,*]

[1]*Chemical Engineering Department, Faculty of Engineering, Universitas Gadjah Mada, Jl. Grafika 2, Kampus UGM, Yogyakarta, 55281, Indonesia*
[2]*Unconventional Georesources Research Center, Faculty of Engineering, Universitas Gadjah Mada, Jl. Grafika 2, Kampus UGM, Yogyakarta, 55281, Indonesia*
[3]*Research Center for Chemistry, National Research and Innovation Agency (BRIN), Kawasan PUSPITEK, Building 452, Serpong, South Tangerang, 15314, Indonesia*
[*]*Corresponding author: yuni_kusumastuti@ugm.ac.id; Tel.: +62-274-555320*

Abstract: This study aimed to synthesize magnetite mesoporous silica nanoparticles using local iron sand obtained from natural resources as magnetite core. The process was carried out in four stages, namely synthesis of magnetite nanoparticles, coating with silica, surfactant templating, silica incorporation, and surfactant removal. The particles were characterized by Scanning Electron Microscopy-Energy Dispersive X-ray spectroscopy (SEM-EDX), X-ray Diffraction (XRD), Particle Size Analyzer (PSA), Vibrating Sample Magnetometer (VSM), Fourier Transform Infrared (FTIR), and Brunauer-Emmett-Teller (BET). The results showed that magnetite mesoporous silica nanoparticles with a 2 g concentration of CTAB contained Fe_3O_4 and SiO_2 compounds, without the chemical bonds related to CTAB. This material showed a smaller particle size distribution of 698.0 nm and a larger saturation magnetization value of 4.76 emu/g, with paramagnetic properties. Furthermore, the surface area, average pore diameter, and volume were 912.950 m^2/g, 3.0706 nm (mesoporous), and 0.83 cm^3/g, respectively. These magnetite mesoporous silica nanoparticles showed potential for application as hyperthermia agents and drug carriers to specific locations.

Keywords: Drug carrier; Iron sand; Magnetite nanoparticles; Mesoporous silica; Surfactant removal

1. Introduction

The concept of nanotechnology is frequently applied to modern developments, offering designed nanomaterials with significant potential to enhance product specifications (Marques et al., 2021). Despite the widespread application, there is no precise definition of nanomaterials in the literature, leading to varied understanding (Baig et al., 2021). Based on the metric system, the nanoscale is a range of value below 1 micrometer (1μm) (European Commission, 2010). In drug delivery applications, nanomaterials serve as carriers to organs, tissue, and cells in the body through blood circulation, allowing direct effect on targeted disease sites. These materials have a unique capability to accumulate in tumor tissues through the enhanced permeability and retention (EPR) effects (Wibowo et al., 2021). Additionally, nanomaterials can be used as hyperthermia agents such as magnetite (Fe_3O_4) nanoparticles.

This work was supported by the Universitas Gadjah Mada funded by Final Project Recognition Grant number 5722/UN1.P.III/Dit-Lit/PT.01.05/2022

https://doi.org/10.14716/ijtech.v16i2.6477
Received May 2023; Revised July 2023; Accepted August 2023

Recently, magnetite nanoparticles have shown potential for diverse applications due to their distinctive properties, including small size, superparamagnetic, low toxicity, and high biocompatibility (Perdani et al., 2020). The unique characteristic of magnetite nanoparticles is the ability to bind with drugs or other biomolecular agents, transfer to the body, and accumulate in targeted cells by magnetic field induction. This therapy produces localized heating in the targeted cell site without overheating the surrounding healthy tissue (Norouzi et al., 2017). However, magnetite nanoparticles have a high surface energy, causing smaller particles to aggregate which can lead to decreased magnetic power and dispersibility. This shows the need for further functionalization and modifications with certain materials such as silica, polymers, carbon, or other metal oxide sorbents (Shen et al., 2018). A practical use of these modified magnetite nanoparticles is in drug delivery applications such as doxorubicin (DOX). Moreover, DOX is a versatile chemotherapy medication extensively used in the treatment of leukemia and various solid tumors, including cancer of the liver, breast, ovarian, and others (Kalyanaraman, 2020).

Silica is a fundamental primary substance that has been used in semiconductors, ceramics, and polymers, including in diverse sectors such as rubber production and pharmaceuticals (Dhaneswara et al., 2020). For pharmaceuticals or biomedical applications, mesoporous silica is a new generation of inorganic materials characterized by ordered porous structure, tuneable particle size, with large pore volume (2-50 nm) and surface area (Baig et al., 2021). The synthesis of mesoporous materials can be carried out by soft templating method using surfactants as soft templates (Baig et al., 2021). During this process, organic surfactant molecules play an important role as structure-directing agents (templates) in producing porosity within the blocks (Cheng et al., 1995). Surfactants in the matrix must be removed to obtain materials with mesoporous structure, large surface area, and pore volume (Cauda et al., 2011). The removal process can be performed by various methods, such as calcination, which has very high surfactant removal efficiency (Ghaedi and Zhao, 2022).

In Indonesia, Glagah Beach, Kulon Progo, Special Region of Yogyakarta, is an area with potential iron sand resources, offering significant opportunities for the synthesis of advanced materials. Despite its preference as a site due to the abundance of iron sand, the potential of Glagah Beach has been optimally realized (Swastika et al., 2021; Putri et al., 2020). Swastika et al. (2021) successfully synthesized Glagah Beach iron sand using the coprecipitation method with variations in HCl concentration (Swastika et al., 2021). Prasetyowati et al., (2021) also synthesized and characterized magnetite nanoparticles based on Glagah Beach iron sand using the coprecipitation method at various concentrations of NH_4OH precipitating solution. Furthermore, Putri et al., (2020) explored the influence of sonication time and size of this iron sand in the preparation process to produce magnetite nanoparticles by ultrasonic radiation method. Prasetyowati et al., (2019) investigated the effect of dissolving iron sand extract in HCl solution on lattice parameters and magnetic properties of magnetite nanoparticles. Moreover, other iron sand resources from Tulungagung Beach, East Java, Indonesia, have been investigated for the synthesis of magnetite/silica nanocomposite (Taufiq et al., 2020). The application of magnetite/silica nanocomposite as a useful material has been conducted by some researchers (Elmaria et al., 2024; Maulana et al., 2024; 2023; Elmaria and Jenie, 2021; Fitri et al., 2019).

Several investigations have been carried out on magnetite mesoporous silica nanoparticles as a drug carrier. However, the investigations only focused on the synthesis of magnetite nanoparticles based on iron sand from Glagah Beach to explore the characteristics of the particles produced. This shows the need to develop a method for producing magnetite mesoporous silica nanoparticles, which can act as a multifunctional platform for hyperthermia agents and drug carriers in future medical applications. Therefore, this study aimed to synthesize magnetite mesoporous silica nanoparticles using local iron sand with cetyltrimethylammonium bromide (CTAB) as a surfactant source. By investigating the effect of cationic surfactants on silica nanoparticles, Singh et al. (2011) found that CTAB produced the smallest particle size. The results provided valuable information regarding particle characteristics of each stage of the synthesis process.

2. Methods

2.1. Materials

Iron sand was obtained from Glagah Beach, Kulon Progo, Special Region of Yogyakarta (S7°54'45.8" E110°3'59.5"). Hydrochloric acid (HCl, 37%), ammonium hydroxide (NH_4OH, 25%), ethanol absolute (C_2H_5OH, 99%), cetyltrimethylammonium bromide (CTAB, 99%), and tetraethyl orthosilicate (TEOS) were purchased from Merck, Germany. All chemicals were used without processing and distilled water was applied during the synthesis process.

2.2. Synthesis of magnetite nanoparticles (Fe_3O_4)

Iron sand obtained from Glagah Beach was sieved first with a sieve size of 140 mesh. Subsequently, 10 g of sample was dispersed into 54 mL of 37% HCl for 2 hours using a sonicator at room temperature. The suspension was filtered using filter paper and the filtrate was dripped with 25% NH_4OH solution gradually until a black precipitate formed, which was separated, washed, and dried.

2.3. Coating of magnetite nanoparticles with silica ($Fe_3O_4@SiO_2$)

A total of 0.4 g of Fe_3O_4 particles were dissolved into 80 mL ethanol, 20 mL distilled water, and 2.5 mL 25% NH_4OH solution, followed by dispersion using a sonicator for 1 hour. Subsequently, 0.8 mL of TEOS was slowly added to the mixture, stirred for 6 hours, and the suspension was separated, washed, and dried.

2.4. Surfactant templating and silica incorporation onto magnetite/silica composite ($Fe_3O_4@SiO_2@CTAB/SiO_2$)

The method of surfactant templating and silica incorporation onto magnetic/silica nanocomposite was conducted based on Kurniasari (2023). A total of 0.4 g of $Fe_3O_4@SiO_2$ particles were dissolved into 250 mL of ethanol and 5 mL of 25% NH_4OH solution, dispersed for 30 minutes, and referred to as solution X. CTAB concentration variations of 1 and 2 g were dissolved in 350 mL distilled water and stirred for 30 minutes, namely solution Y. Subsequently, solution X and Y were mixed, stirred for 4 hours at room temperature, and added with 4 mL of TEOS at varying stirring times of 20 and 120 minutes, respectively. The solution was maintained at a constant temperature of 35°C, while the suspension obtained was separated, washed, and dried.

2.5. Surfactant removal ($Fe_3O_4@SiO_2@SiO_2$)

A total of 1 g of $Fe_3O_4@SiO_2@CTAB/SiO_2$ particles were calcined using a furnace at 350°C for 3 hours. The sample matrix conducted in this study and illustration of each stage for magnetite mesoporous silica nanoparticles preparation are presented in Table 1 and Figure 1.

Table 1 Research sample matrix

Particles	CTAB concentration (grams)	Silica formation reaction time (minutes)	Sample
Fe_3O_4	-	-	A
$Fe_3O_4@SiO_2$	-	-	B
$Fe_3O_4@SiO_2@SiO_2$	1	20	C
$Fe_3O_4@SiO_2@SiO_2$	1	120	D
$Fe_3O_4@SiO_2@SiO_2$	2	120	E

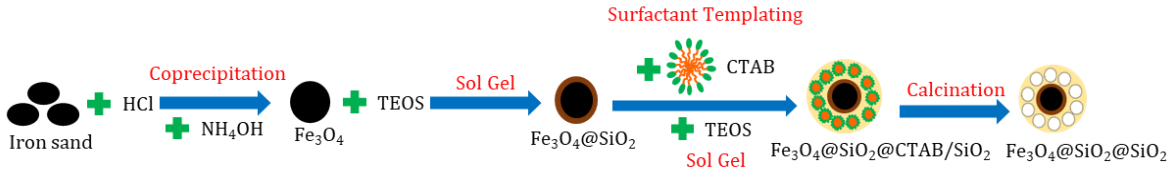

Figure 1 Illustration of each stage for magnetite mesoporous silica nanoparticles preparation

2.6. Characterization

In this study, X-ray Diffraction (XRD) Rigaku Type Smartlab X-ray Difratometer 40kVa was used to analyze the crystallinity (Lin et al., 2014). Scanning Electron Microscopy (SEM) was used as a standard method for direct imaging and dimensional measurement of micro and nano structures (Torres-Rivero et al., 2021). Energy Dispersive X-ray spectroscopy (EDX) was used for elemental analysis and chemical characterization of samples (Patra and Baek, 2014). Specifically, the type of SEM-EDX instrument used was JEOL JSM-6510LA. Particle Size Analyzer (PSA) Horiba SZ-100 was used to measure particle size distribution, while Fourier Transform Infrared (FTIR) Shimadzu A224158 spectroscopy was applied to identify functional groups presented in the form of spectra (Patra and Baek, 2014). The Brunauer-Emmett-Teller (BET) Quantachrome NovaWin Instruments v11.03 analysis was used to identify surface area, pore size, and volume of materials (Jaroniec et al., 1998). Vibrating Sample Magnetometer (VSM) VSM250 is a characterization method to determine the magnetic properties of a sample (Kirupakar et al., 2016).

3. Results and Discussion

3.1. SEM Analysis

Iron sand, which had been transformed into a magnetite nanoparticle, was characterized using SEM analysis to observe the size and morphology. Based on Figure 2, magnetite nanoparticles showed a tendency to agglomerate due to the magnetic interaction (Moorthy et al., 2017).

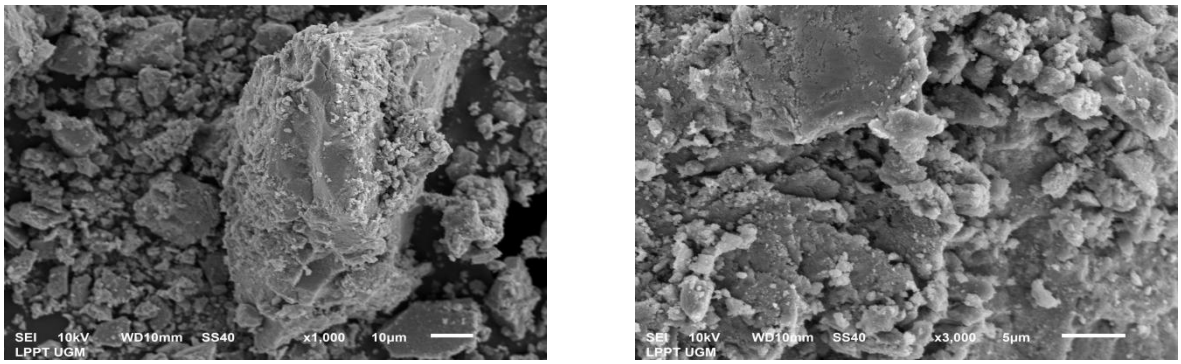

Figure 2 SEM analysis results on magnetite nanoparticles

3.2. EDX Analysis

Based on the elemental composition presented in Table 2, impurities such as Al, Si, and Ca in sample A showed significant reduction compared to iron sand. Meanwhile, Fe content increased from 67.81% to 76.58% in sample A due to the co-precipitation process that can produce magnetite nanoparticles with higher Fe content and fewer impurities. These results showed that local iron sand from Glagah Beach could be used as magnetite nanoparticles.

Table 2 Composition of iron sand and magnetite nanoparticles

Element	Mass, %	
	Iron Sand	Sample A
C	3.06	3.87
O	26.8	18.53
Al	0.69	0.53
Si	0.76	0.11
Ca	0.88	0.38
Fe	67.81	76.58
Total	100	100

3.3. XRD Analysis

The phase, crystallite size, crystal shape, and elemental composition of the samples were characterized using XRD analysis. In Figure 3, for sample A, the diffraction peaks 2θ = 30°, 35°, 43°, 53°, 57°, and 63° were observed, serving as characteristic of Fe_3O_4 according to JCPDS 19-0629, with index miller [220], [311], [400], [422], [511], and [440] planes (Moorthy et al., 2017). In sample B, the diffraction peak 2θ = 22°-27° was observed, showing the presence of silica with an amorphous phase (Taufiq et al., 2020). Magnetite diffraction peaks were also found in sample B, indicating that silica successfully coated the Fe_3O_4 magnetite core. In samples D and E, a broadening of the silica diffraction peak was identified, which was related to the presence of large pores in the material (Purwaningsih et al., 2019). This showed that there were large pores formed in the silica due to the effect of the surfactant templating process using CTAB, requiring further quantification by BET analysis.

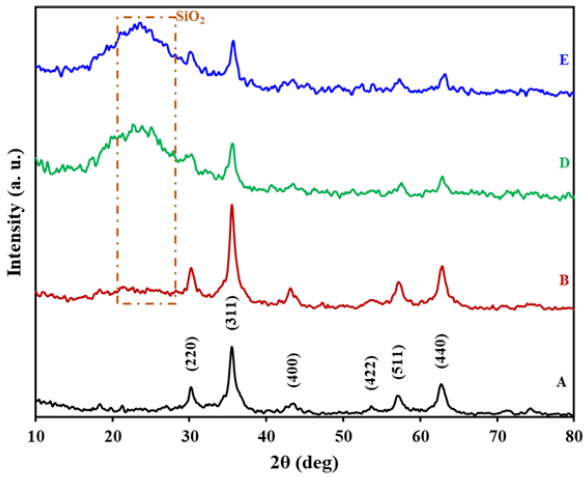

Figure 3 XRD analysis of synthesized particles at each stage

The crystallite size of magnetite nanoparticles was calculated using the Debye-Scherrer equation:

$$D = \frac{k\,\lambda}{\beta\,cos\theta} \quad (1)$$

where D is the crystallite size (nm), k is the shape parameter (for magnetite which is 0.89), λ is the wavelength of X-ray (0.154 rad), β is the full width at half maximum of the peak (FWHM), and θ is the diffraction angle. Subsequently, the crystallite size of samples A and B are shown in Table 3.

Table 3 Average crystal size of sample at each stage

Stage	Sample	Average crystal size (nm)			
		This study	Putri et al. (2020)	Taufiq et al. (2020)	Swastika et al. (2021)
1	A	1.36	2.7-68.8	8.2	22
2	B	1.41	-	8.9-13.2	-

3.4. PSA Analysis

At the stage of surfactant templating and silica incorporation (sol-gel), silica interacted with the hydrophilic component of CTAB through electrostatic forces, as presented in Figure 4 (Semeykina and Zharov, 2022). The type of electrostatic interaction that occurred including silica charge was controlled by pH and isoelectric point, where the molecular charge is zero (Pal and Bhaumik, 2013). Generally, silica species have an isoelectric point of 2, showing a positive, neutral, and negative charge in acidic (pH<2), neutral (pH=2), and alkaline (pH>2) conditions, respectively. At the end of the surfactant templating and silica incorporation into the magnetite/silica composite stage, a

solution with pH 9 was formed due to the addition of NH_4OH. Therefore, the condition of the solution was alkaline, making the silica negatively charged. To determine the type of electrostatic interaction, the inorganic precursor was symbolized as I and the polar head of the surfactant was denoted as S. In this study, silica is negatively charged and CTAB is a cationic surfactant making it positively charged. Consequently, the type of electrostatic interaction that occurs is the S^+I^- interaction. The type of interaction to produce well-organized mesoporous silica material is the S^+I^- (alkaline conditions) and $S^+X^-I^+$ (acidic conditions) (Xiang et al., 2010).

Table 4 shows the particle size data of all samples in this study based on PSA analysis. The presence of the silica coating stage on magnetite nanoparticles caused the particle size of sample B to be 114.6% or 2.15 times larger than A. At the same CTAB concentration of 1 g, sample D produced a larger particle size than sample C. This showed that prolonged reaction time resulted in a longer silica growth process, leading to a larger particle size. Sample C was also studied to determine the extent of silica growth from 20 minutes to 120 minutes (sample D). However, the increase in particle size that occurred was significant at 17.62%.

At the same complete reaction time of 120 minutes, sample E had a smaller particle size than sample D. This showed that a larger concentration of CTAB led to smaller particle size, causing the formation of more micelles, and increasing the bonds between silica and CTAB. Therefore, the bonds between silica and silica to form Si-O-Si groups would decrease, resulting in smaller particle size (Purwaningsih et al., 2019).

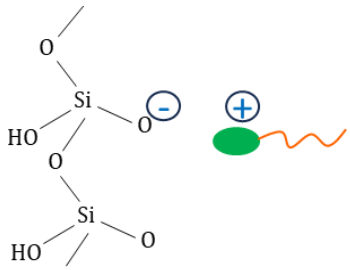

Figure 4 Illustration of the interaction between CTAB and silica

Table 4 Particle size distribution of the synthesized results at each stage

Sample	Particle size (nm)
A	213.8
B	459.0
C	629.4
D	740.3
E	698.0

3.5. VSM Analysis

The magnetic properties of a material can be measured using a Vibrating Sample Magnetometer (VSM). Figure 5 shows that samples A and B have superparamagnetic properties, indicated by remnant magnetization (Mr) and coercivity field (Hc) values that are close to zero, and high saturation magnetization (Ms) values (Taufiq et al., 2020; Quy et al., 2013). Meanwhile, the type of hysteresis loop of samples D and E has paramagnetic properties.

Ms, Mr, and Hc values of all samples are presented in Table 5. A comparison of samples A and B shows a decrease in Ms value due to non-magnetic surface coating by silica (Moorthy et al., 2017). Due to the smaller particle size, sample E has a slightly higher Ms value than sample D From the results of VSM analysis, a higher concentration of CTAB can provide magnetic strength with a larger saturation magnetization value.

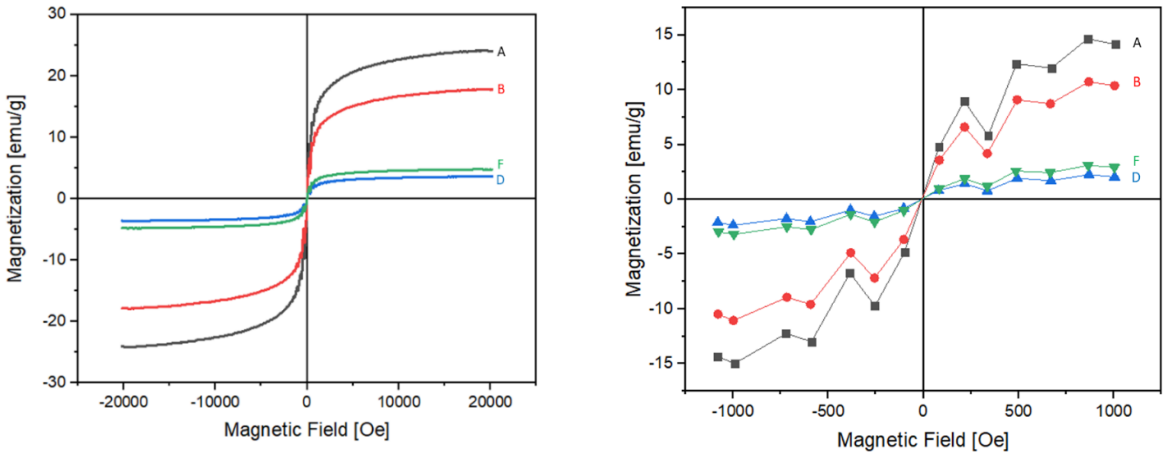

Figure 5 Magnetization curves of particles synthesized with magnetic field range of (a) ±20.000 Oe (b) ±1.000 Oe

Table 5 Ms, Mr, and Hc values of particles synthesized at each stage from magnetization data analysis

Stage	Sample	This study		
		Ms [emu/g]	Mr [emu/g]	Hc [Oe]
1	A	24.04	0.447	-8.42
2	B	17.78	0.347	-8.91
4	D	3.60	0.095	-9.23
4	E	4.76	0.099	-10.73

3.6. FTIR Analysis

FTIR analysis was performed to confirm the formation of silica in magnetite nanoparticles and the removal of CTAB surfactant in the synthesized particles. Based on the results of PSA and VSM analysis, sample E was used in FTIR analysis due to its smaller size and higher MS value compared to sample D. From Figure 6, the characteristic peak appearing at 590 cm^{-1} in the sample confirmed the presence of Fe_3O_4. The vibration peak at 559 cm^{-1} showed the presence of SiO_2 coating to the Fe_3O_4 magnetite core. The vibrational bands at 802 cm^{-1} and 971 cm^{-1} were identified as Si-OH bonds, while 1061 cm^{-1} showed Si-O-Si bonds. This showed the formation of silica network and surface silanol groups. Additionally, Figure 6 showed no wavenumber for the chemical bonds of CH-, $N(CH_3)_2$, $-CH_2-$, indicating that the CTAB removal process by calcination at 350°C was successful. This suggested a high template removal efficiency and ability to minimize the particle structural damage.

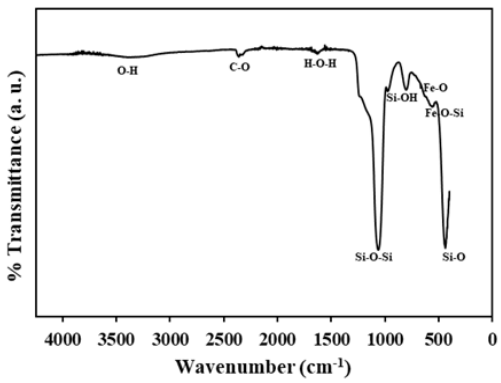

Figure 6 FTIR analysis of magnetite mesoporous silica nanoparticles (sample E)

3.7. BET Analysis

The surface area of sample E was very high, approximately 912.950 m^2/g, with an average pore diameter of 3.0706 nm and volume of 0.83 cm^3/g. The molecular size of DOX was estimated to be 1.5 nm (Bilalis et al., 2016). Due to an average pore diameter of 3.0706 nm, the anticancer drug DOX can fit into the pores of these magnetite mesoporous silica nanoparticles.

3.8. Magnetism Suspension Test

The magnetism test of the suspension of magnetite mesoporous silica nanoparticles (sample E) in water was carried out as shown in Figure 7. The results showed that the synthesized particles, namely magnetite mesoporous silica nanoparticles, could be directed by an external magnetic field,

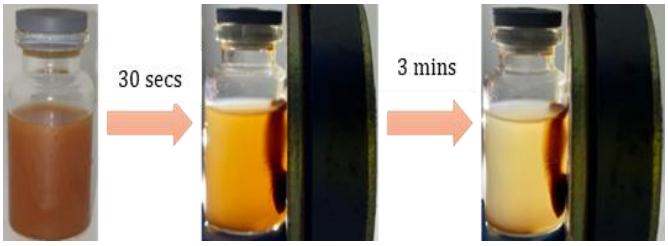

Figure 7 Magnetism test of magnetite mesoporous silica nanoparticle suspension in water (sample E)

4. Conclusions

In conclusion, this study showed the synthesis of magnetite mesoporous silica nanoparticles from local iron sand of Glagah Beach as a potential drug carrier. Based on EDX analysis results, the purity of Fe_3O_4 produced was 76.58%, showing that local iron sand from Glagah Beach could be used as magnetite nanoparticles. Sample E (Fe_3O_4@SiO_2@SiO_2 particles) with a higher CTAB concentration, had a smaller particle size with a surface area of 912.950 m^2/g, and an average pore diameter of 3.0706 nm. Additionally, sample E had a higher Ms value, paramagnetic properties, and could be directed by an external magnetic field, with potential as a hyperthermia agent. These results showed that Fe_3O_4 magnetite nanoparticles from iron sand Glagah Beach Yogyakarta were successfully synthesized into magnetite mesoporous silica nanoparticles (Fe_3O_4@SiO_2@SiO_2), showing significant potential for future biomedical applications.

Acknowledgements

This work was supported by the Universitas Gadjah Mada funded by Final Project Recognition Grant number 5722/UN1.P.III/Dit-Lit/PT.01.05/2022.

Author Contributions

Mita Kurniasari: Experiments, analysis, writing. Himawan Tri Bayu Murti Petrus: Supervision. Siti Nurul Aisyiyah Jenie: Analysis and revision. Yuni Kusumastuti: Conceptualization, revision and correction.

Conflict of Interest

The authors have no conflicts of interest to declare.

References

Baig, N, Kammakakam, I & Falath, W 2021, 'Nanomaterials: A review of synthesis methods, properties, recent progress, and challenges', *Materials Advances*, vol. 2, no. 6, pp. 1821-1871, https://doi.org/10.1039/D0MA00807A

Bilalis, P, Tziveleka, LA, Varlas, S & Iatrou, H 2016, 'pH-Sensitive nanogates based on poly(l-histidine) for controlled drug release from mesoporous silica nanoparticles', *Polymer Chemistry*, vol. 7, no. 7, pp. 1475-1485, https://doi.org/10.1039/C5PY01841B

Cauda, V, Argyo, C, Piercey, DG & Bein, T 2011, '"Liquid-phase calcination" of colloidal mesoporous silica nanoparticles in high-boiling solvents', *Journal of the American Chemical Society*, vol. 133, no. 17, pp. 6484-6486, https://doi.org/10.1021/ja1067492

Cheng, CF, Luan, Z & Klinowski, J 1995, 'The role of surfactant micelles in the synthesis of the mesoporous molecular sieve MCM-41', *Langmuir*, vol. 11, no. 7, pp. 2815-2819, https://doi.org/10.1021/la00007a075

Dhaneswara, D, Fatriansyah, JF, Situmorang, FW & Haqoh, AN 2020, 'Synthesis of amorphous silica from rice husk ash: Comparing HCl and CH_3COOH acidification methods and various alkaline concentrations', *International Journal of Technology*, vol. 11, no. 1, pp. 200-208, https://doi.org/10.14716/ijtech.v11i1.3335

Elmaria, FA & Jenie, SNA 2021, 'Magnetic nanoparticles based on natural silica as a methyl ester forming acid catalyst', *Indonesian Journal of Applied Chemistry*, vol. 23, no. 2, pp. 49-54

Elmaria, FA, Aulia, F, Hidayati, LN, Kristiani, A, Sudiyarmanto, Kusumastuti, Y, Jenie, SNA & Petrus, HTMB 2024, 'Facile synthesis of magnetic-fluorescent iron oxide-geothermal silica core/shell nanocomposites via modified sol-gel method', *Journal of Sol-Gel Science and Technology*, vol. 110, pp. 1-10. https://doi.org/10.1007/s10971-024-06318-8

European Commission 2010, *Scientific basis for the definition of the term "nanomaterial"*, Scientific Committee on Emerging and Newly Identified Health Risks, July, pp. 1-43

Fitri, WA, Sururoh, L & Jenie, SNA 2019, 'The effect of calcination temperature on the synthesis of magnetic silica nanoparticles from geothermal sludge', *AIP Conference Proceedings*, vol. 2175, no. 1, https://doi.org/10.1063/1.5134644

Ghaedi, H & Zhao, M 2022, 'Review on template removal techniques for synthesis of mesoporous silica materials', *Energy and Fuels*, vol. 36, no. 5, pp. 2424-2446, https://doi.org/10.1021/acs.energyfuels.1c04435

Jaroniec, M, Kruk, M, Sayari, A 1998, 'Adsorption methods for characterization of surface and structural properties of mesoporous molecular sieves', Studies in Surface Science and Catalysis, vol. 117, pp. 325-332, https://doi.org/10.1016/S0167-2991(00)80261-X

Kalyanaraman, B 2020, 'Teaching the basics of the mechanism of doxorubicin-induced cardiotoxicity: Have we been barking up the wrong tree?', *Redox Biology*, vol. 29, p. 101394, https://doi.org/10.1016/j.redox.2019.101394

Kirupakar, B, R, Vishwanath, Dr.B.A, Padma Sree, M, Deenadayalan 2016, ' Vibrating sample magnetometer and its application in characterisation of magnetic property of the anti cancer drug magnetic microspheres', *International Journal of Pharmaceutics & Drug Analysis, vol*. 4, pp. 227-233, https://www.ijpda.org/index.php/journal/article/view/223

Kurniasari, M 2023, *Effect of Cetyltrimethylammonium Bromide (CTAB) as surfactant-template on the synthesis of magnetite mesoporous silica nanoparticles* (Master's thesis), Universitas Gadjah Mada

Lin, PC, Lin, S, Wang, PC & Sridhar, R 2014, 'Techniques for physicochemical characterization of nanomaterials', *Biotechnology Advances*, vol. 32, no. 4, pp. 711-726, https://doi.org/10.1016/j.biotechadv.2013.11.006

Marques, AC, Vale, M, Vicente, D, Schreck, M, Tervoort, E & Niederberger, M 2021, 'Porous silica microspheres with immobilized titania nanoparticles for in-flow solar-driven purification of wastewater', *Global Challenges*, vol. 5, no. 5, p. 2000116, https://doi.org/10.1002/gch2.202000116

Maulana, MY, Raissa, R, Nurrudin, A, Andreani, AS, Angelina, M, Septiani, NLW, Yuliarto, B & Jenie, SNA 2024, 'An ultra-sensitive SARS-CoV-2 antigen optical biosensor based on angiotensin converting enzyme 2 (ACE-2) functionalized magnetic-fluorescent silica nanoparticles', *Nanotechnology*, vol. 35, no. 20, p. 205702, https://doi.org/10.1088/1361-6528/ad27aa

Maulana, MY, Yuliarto, B, Jenie, SNA & Septiani, NLW 2023, 'Comparative X-ray diffraction (XRD) study on the synthesis of natural based magnetic silica nanoparticles', *Journal of Metastable and Nanocrystalline Materials*, vol. 35, pp. 25-31, https://doi.org/10.4028/p-6d8vlt

Moorthy, MS, Bharathiraja, S, Manivasagan, P, Lee, KD & Oh, J 2017, 'Crown ether triad modified core-shell magnetic mesoporous silica nanocarrier for pH-responsive drug delivery and magnetic hyperthermia applications', *New Journal of Chemistry*, vol. 41, no. 19, pp. 10935-10947, https://doi.org/10.1039/C7NJ02432K

Norouzi, M, Nazari, B & Miller, DW 2017, 'Electrospun-based systems in cancer therapy', *Electrospun Materials for Tissue Engineering and Biomedical Applications: Research, Design and Commercialization*, Elsevier Ltd, pp. 337-356, https://doi.org/10.1016/B978-0-08-101022-8.00013-2

Pal, N & Bhaumik, A 2013, 'Soft templating strategies for the synthesis of mesoporous materials: Inorganic, organic-inorganic hybrid and purely organic solids', *Advances in Colloid and Interface Science*, vol. 189-190, pp. 21-41, https://doi.org/10.1016/j.cis.2012.12.002

Patra, JK & Baek, KH 2014, 'Green nanobiotechnology: Factors affecting synthesis and characterization techniques', *Journal of Nanomaterials*, vol. 2014, pp. 1-12, https://doi.org/10.1155/2014/417305

Perdani, MS, Juliansyah, MD, Putri, DN, Utami, TS, Hudaya, C, Yohda, M & Hermansyah, H 2020, 'Immobilization of cholesterol oxidase in chitosan magnetite material for biosensor application', *International Journal of Technology*, vol. 11, no. 4, pp. 754-763, https://doi.org/10.14716/ijtech.v11i4.2852

Prasetyowati, R, Ariswan, W & Dewi, N 2019, 'Synthesis and characterization of magnetite nanoparticles (Fe_3O_4) based on iron sand from Glagah Kulon Progo Yogyakarta via coprecipitation method with variations in the dissolution duration', *The Science and Science Education International Seminar Proceedings*, vol. 2019, pp. 1-10

Prasetyowati, R, Widiawati, D, Swastika, PE, Ariswan, A & Warsono, W 2021, 'Synthesis and characterization of magnetite (Fe3O4) nanoparticles based on iron sands at Glagah Beach Kulon Progo with coprecipitation methods at various NH4OH concentrations', *Jurnal Sains Dasar*, vol. 10, no. 2, pp. 57-61

Purwaningsih, H, Ervianto, Y, Pratiwi, VM, Susanti, D & Purniawan, A 2019, 'Effect of cetyl trimethyl ammonium bromide as template of mesoporous silica MCM-41 from rice husk by sol-gel method', *IOP Conference Series: Materials Science and Engineering*, vol. 515, no. 1, p. 012052, https://doi.org/10.1088/1757-899X/515/1/012051

Putri, NRE, Firdausi, SI, Najmina, M, Amelia, S, Timotius, D, Kusumastuti, Y & Petrus, HTBM 2020, 'Effect of sonication time and particle size for synthesis of magnetic nanoparticle from local iron sand', *Journal of Engineering Science and Technology*, vol. 15, no. 2, pp. 894-904

Quy, DV, Hieu, NM, Tra, PT, Nam, NH, Hai, NH, Son, NT, Nghia, PT, Anh, NTV, Hong, TT & Luong, NH 2013, 'Synthesis of silica-coated magnetic nanoparticles and application in the detection of pathogenic viruses', *Journal of Nanomaterials*, vol. 2013, pp. 1-6, https://doi.org/10.1155/2013/603940

Semeykina, V & Zharov, I 2022, 'Medium controlled aggregative growth as a key step in mesoporous silica nanoparticle formation', *Journal of Colloid and Interface Science*, vol. 615, pp. 236-247, https://doi.org/10.1016/j.jcis.2022.01.166

Shen, L, Li, B & Qiao, Y 2018, 'Fe_3O_4 nanoparticles in targeted drug/gene delivery systems', *Materials*, vol. 11, no. 2, p. 324, https://doi.org/10.3390/ma11020324

Singh, LP, Bhattacharyya, SK, Mishra, G & Ahalawat, S 2011, 'Functional role of cationic surfactant to control the nano size of silica powder', *Applied Nanoscience*, vol. 1, pp. 117-122, https://doi.org/10.1007/s13204-011-0016-1

Swastika, PE, Hardheyanti, F, Prasetyowati, R, Ariswan, A & Warsono, W 2021, 'Effect of HCl concentration of microstructure and magnetic properties of Fe_3O_4 nanoparticles synthesized from iron sand in Glagah Beach Kulonprogo', *Jurnal Sains Dasar*, vol. 10, no. 1, pp. 24-29, http://dx.doi.org/10.21831/jsd.v10i1.39141

Taufiq, A, Nikmah, A, Hidayat, A, Sunaryono, S, Mufti, N, Hidayat, N & Susanto, H 2020, 'Synthesis of magnetite/silica nanocomposites from natural sand to create a drug delivery vehicle', *Heliyon*, vol. 6, no. 4, p. e03739, https://doi.org/10.1016/j.heliyon.2020.e03784

Torres-Rivero, K, Bastos-Arrieta, J, Fiol, N & Florido, A 2021, 'Metal and metal oxide nanoparticles: An integrated perspective of the green synthesis methods by natural products and waste valorization: Applications and challenges', *Comprehensive Analytical Chemistry*, vol. 94, pp. 433-469, https://doi.org/10.1016/bs.coac.2021.04.004

Wibowo, A, Jatmiko, A, Ananda, MB, Rachmawati, SA, Ardy, H, Aimon, AH & Iskandar, F 2021, 'Facile fabrication of polyelectrolyte complex nanoparticles based on chitosan - poly-2-acrylamido-2-methylpropane sulfonic acid as a potential drug carrier material', *International Journal of Technology*, vol. 12, no. 3, pp. 561-570, https://doi.org/10.14716/ijtech.v12i3.4193

Xiang, WD, Yang, YX, Zheng, JL, Cao, L, Ding, HJ & Liu, XN 2010, 'Synthesis of mesoporous silica by cationic surfactant templating in various inorganic acid sources', *Materials Science-Poland*, vol. 28, no. 3, pp. 609-615